FEM MODELING OF PEBBLE BED/STRUCTURAL WALL SEPARATION

Chunbo (Sam) Zhang,* Alice Ying, Mohamed A. Abdou

Fusion Science and Technology Center, University of California, Los Angeles
420 Westwood Plaza, Los Angeles, CA 90095-1597, USA, chunbozhang@fusion.ucla.edu

This work has developed FEM models of ceramic breeder pebble beds and applied them to two categories of blanket design (edge-on and layer configurations) to predict the thermomechanical behavior of a pebble bed under ITER pulsed operating condition. To explore the pebble bed/structural wall separation phenomenon, a thermomechanical contact is considered using contact elements meshed along pebble/structure interface. The pebble bed/wall dynamic contact/separation process has been simulated, and the gap distance distribution and variation have been analyzed and presented. Pebble bed/wall separation occurs during the plasma-off period and varies with both location and time. A maximal radial gap of 0.64mm is found for an edge-on configuration after the 1st ITER cycle within the range of studied parameters. For the layer configuration, a poloidal gap of 1.99mm, larger than the pebble diameter, is found. The generated gap can cause the even large rearrangement of pebbles and result in a disturbed packing during further cycling. Consequently, a design solution is suggested to mitigate this situation.

I. INTRODUCTION

Ceramic breeder pebble beds in test blanket modules (TBM) proposed by ITER parties undergo thermal cycles during ITER pulsed operations. Consequently, pebble bed/wall separation may occur due to the combined effect of thermal expansion/contraction, thermal- or irradiation- (at a later stage) induced creep, pebble rearrangement, and pebble cracking. Understanding of such a separation is critical because the heat transfer efficiency of pebble bed can be significantly reduced. To predict pebble bed/wall separation one requires the knowledge of how the pebble bed and wall interacts thermally and mechanically during operation. However, a predictive capability of gap formation is not yet fully established.[1]

The objective of this work is to develop FEM models using ANSYS computational software[2] to be able to predict and quantify the pebble bed thermomechanical response and the pebble bed/structural wall separation phenomenon under ITER pulsed operations. Initially, we introduced new CAP yielding, hardening and creep material models of pebble beds to the thermomechanical FEM simulations of pebble beds. Moreover, we employ a contact technique in the FEM models to simulate and monitor the contact status between breeder region (pebble bed) and its structural container. Based on the developed FEM models, a pebble bed/wall dynamic and cyclic contact/separation process has been simulated and analyzed for both edge-on and layer configurations. Presented simulation results include the distribution and profile of pebble bed/wall gap distance and the thermomechanical field of pebble bed and its evolution in the existence of gap.

II. FEM MODELING OF PEBBLE BED/WALL SEPARATION

Although pebble-scale simulations are necessary to simulate the dynamic inter-pebble interactions, the huge dimension difference of pebbles and structural container, from a computational standpoint, prohibits models of that scale when analyzing full multi-layer ceramic breeder blanket. Therefore, we have chosen the FEM approach as the tool for pebble bed/wall separation analysis. FEM modeling is able to efficiently predict the bulk thermomechanical behavior of a pebble bed and its interactions with a structural wall for different blanket designs. A fundamental assumption for FEM modeling is that a pebble bed can be treated as a continuous media with effective material properties that can be experimentally identified. Due to the limitations of FEM modeling, the influences of pebble-scale packing, deformation, cracking and rearrangement cannot be simulated. However, their combined and equivalent effects are reflected in the permanent volume change of a pebble bed, which is considered in the developed material models through the calibration with experimental data.

II.A. Material Models with Validation

The mechanical behavior of a pebble bed involves three distinct regimes: 1) a non-linear elastic regime; 2) a cap plasticity/hardening regime; and 3) a strain-hardening creep regime.

II.A.1 Non-Linear Elasticity

The isotropic non-linear elasticity, defined by Eq. (1), is used to describe pebble bed elastic behavior.[3,4] The Young's modulus is a function of two stress invariants, I_1

and J_2, and temperature, T. The material parameters of $A_e(T)$ and s can be identified by experimental data.

$$E = A_e(T)[(1+\nu)J_2 + \frac{1-\nu}{3}I_1^2]^{s/2} + E_0 \qquad (1)$$

II.A.2 Cap Plasticity/Hardening

The cap model embedded in ANSYS is employed to simulate the permanent volume reduction of a pebble bed, including pebble rearrangement, which defines the yield surfaces and their evolution based on the stress state.[2] Compared with other cap models applied to pebble bed study, two features make this cap model distinctive. They are: (1) a single continuous cap yield surface which overcomes the difficulty of transition from compactive to dilatant deformation before shear failure;[5] (2) the hydrostatic-pressure and volumetric-strain relationship (cap hardening law) in an exponential form which can capture a wide range of compaction behavior including one or two inflection points.[6]

The cap model in ANSYS (Ref. 2) consists of shear failure (Y_s) and compaction (Y_c) portions, shown in Fig. 1. This unified and compacted CAP yielding function (Y) is formulated in Eq. (2), and the cap hardening law is defined through a function of volumetric plastic strain (ε_v^p) and I_1, which has the exponential form in Eq. (3). Temperature's effect has been included by defining the temperature-dependent parameters of Ae and W in Eqs. (1) and (3).

$$Y(I_1, J_2, K, \sigma_0) = J_2 - Y_c(I_1, K, \sigma_0)Y_s^2(I_1, \sigma_0) \qquad (2)$$

$$Y_s(I_1, \sigma_0) = \sigma_0 - \alpha I_1$$

$$Y_c(I_1, K, \sigma_0) = 1 - H(K - I_1)[\frac{I_1 - K}{RY_s(K, \sigma_0)}]^2$$

$$\varepsilon_v^p = W(T)\{e^{[D_1 - D_2(X - X_0)](X - X_0)} - 1\} \qquad (3)$$

II.A.3 Strain-Hardening Creep Model

To better predict the creep deformation of a pebble bed affected by temperature/stress distribution and evolution, a strain-hardening creep model is chosen, in

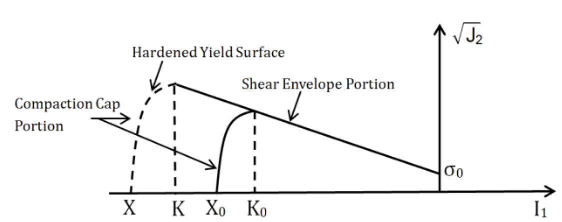

Fig. 1. Schematic of CAP model.

which the volumetric creep strain rate ($\dot{\varepsilon}_{v,cr}$) is expressed as a function of equivalent creep stress ($\overline{\sigma}_{cr}$), volumetric creep strain ($\varepsilon_{v,cr}$) and temperature (T), shown in Eq. (4).[2] C_1-C_4 are material constants.

$$\dot{\varepsilon}_{v,cr} = C_1 \overline{\sigma}_{cr}^{C_2} \varepsilon_{v,cr}^{C_3} e^{-C_4/T} \qquad (4)$$

Figure 2 illustrates the validation of the developed material models for a Li_4SiO_4 pebble bed by comparing the simulation results with experimental data of uniaxial compaction tests,[7,8] including the pebble bed stress-strain relation and creep evolution for a wide stress/temperature range. A good agreement is achieved.

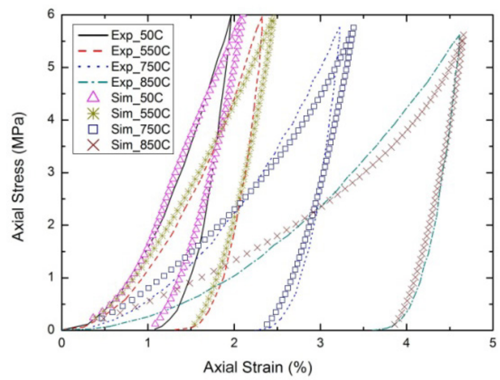

(a)

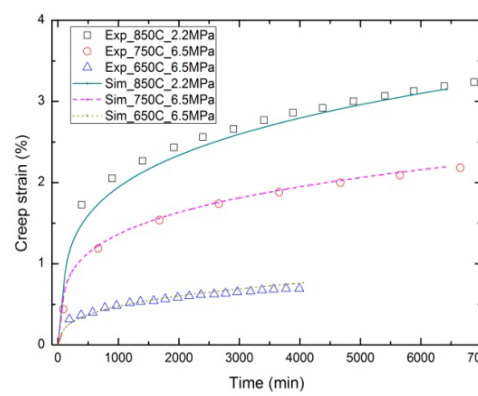

(b)

Fig. 2. Comparisons of Li_4SiO_4 pebble bed stress-strain relation (a) and creep evolution (b) between FEM model prediction and experimental data.

II.B. Model Geometry and Simulation Conditions

Modeling geometries and boundary conditions of edge-on and layer configurations are shown in Fig. 3. For edge-on configuration, the pebble bed has a dimension of 238.5mm × 25.4mm, and 670mm×20mm for layer configuration. For both cases, a fixed B.C. indicated in Fig. 3, coolant bulk temperature (300°C for edge-on and 400°C for layer) and convective heat transfer (1500W/m^2-K) for cooling channels are applied. The edge-on case has a surface heat flux (0.5MW/m^2) on the first wall (FW) and volumetric heat flux exponentially decreasing along the radial direction. The layer case has only the volumetric heat flux with a parabolic distribution along the radial direction. The thermomechanical properties of ferritic steel are used for the structural walls. The correlation of effective thermal conductivity of a Li_4SiO_4 pebble bed as a function of temperature is used.[9]

Pebble bed/wall thermomechanical interactions have been simulated by meshing their interface with contact elements. Due to the lack of a temperature-dependent pebble bed/wall friction coefficient, a constant value of 0.035 is used.[10] A heat transfer coefficient for the Li_4SiO_4/stainless steel interface of 4000W/m^{2}K is applied to pebble bed/wall thermal contact simulation, and He gas thermal conductivity is used for pebble bed/wall gap.[11,12] The plasma cycle follows the ITER operation condition, 400s plasma-on and 1400s plasma-off. Gravity's effect is considered in the layer configuration, but not in the edge-on configuration. The structural container works in its elastic regime. Influences of irradiation and purge gas flow are not included.

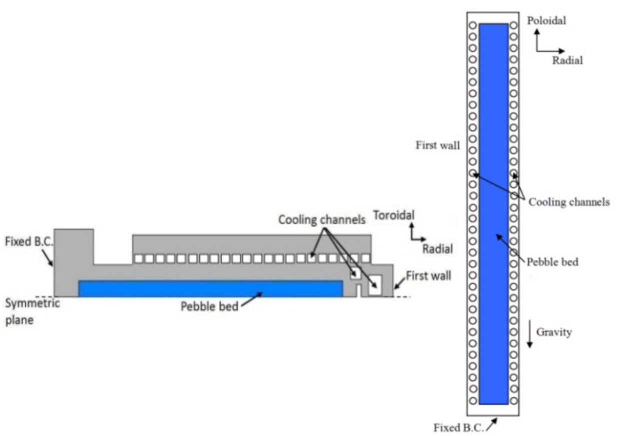

Fig. 3. FEM model geometry: (a) edge-on configuration; (b) layer configuration.

III. SIMULATION RESULTS AND DISCUSSIONS

It should be noted that the prediction of pebble bed deformation strongly depends on the experimental data used for the calibration of pebble bed material models. The elastic strain in FEM reflects the volume change of pebble bed due to pebble's elastic deformation and dilatancy effect. While the inelastic strain (plastic + creep) in FEM represents the permanent bed volume change resulting from the force-initiated pebbles rearrangement, inelastic deformation, cracking, etc.

III.A. Thermomechanical Field Distribution and Evolution of Pebble Bed

Since pebble bed/wall separation is the result of pebble bed volume reduction, it is necessary to analyze the thermomechanical field of the pebble bed, especially pebble bed deformation. Figures 4 and 5 illustrate the temperature, stress and strain distributions of the pebble beds at the end of the 1st heating period (t=400s). For both configurations, a hot zone occurs inside pebble bed with the peak temperatures of 797°C (edge-on) and 882°C (layer). Due to pebble bed thermal expansion, compressive stress/strain concentrates inside pebble bed as well, and decreases away from its center. By comparison, the layer configuration has a concentrated temperature/stress/strain zone throughout the bed, while the concentrations in edge-on configuration are confined to a smaller region near the FW. A higher compressive stress is predicted for the edge-on configuration, but the layer configuration results in a larger inelastic (plastic + creep) strain, for which more pebble bed volume reduction is expected. The other direction has similar stress values, and smaller strain values due to large dimension differences.

Figure 6 shows that pebble bed temperature increases during heating period and thereafter drops to the coolant temperature at about 1000s. However, the thermal-induced stress increases first and decreases during the heating period, which starts at about 250s. Stress

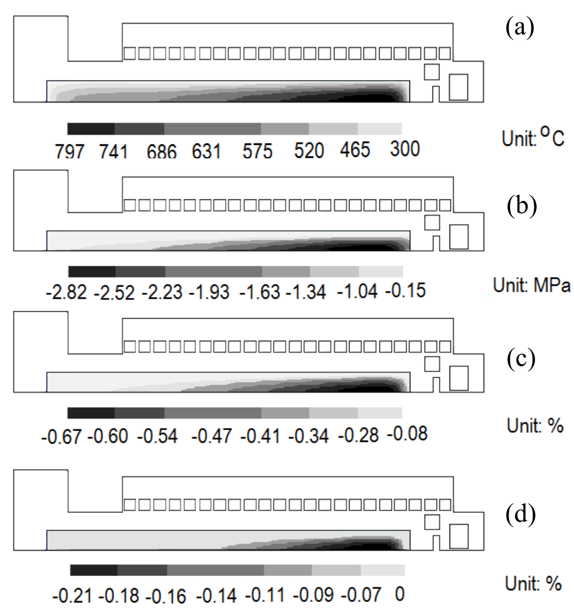

Fig. 4. Thermomechanical field distribution of Li_4SiO_4 pebble bed at the end of 1st heating period (t=400s) for edge-on configuration: (a) temperature; (b) radial stress; (c) radial plastic strain; (d) radial creep strain.

relaxation is caused by pebble bed inelastic deformation and, within the range of studied parameters, observed only when pebble bed creep effect is considered in modeling, which means that the inelastic deformation is high enough to affect the stress trend. For the case when the creep effect is not considered, the stress will keep increasing during the entire heating period and drop when the cooling period starts (t=400s). Since pebble bed/wall separation occurs during the cooling period (t=450s) in Fig. 8, compressive stress quickly drops once the gap is generated and saturates after about 500s. With continuous plasma burn cycles, stress among pebble beds will be further relaxed due to more pebble bed volume shrinkage and finally saturate after a certain number of cycles. The sources of stress relaxation come mainly from the pebble's plastic/creep deformation in FEM modeling.

III.B. Pebble Bed/Wall Gap Distance Distribution and Evolution

Simulation results of pebble bed/wall separation are presented in Figs. 7-9, which include the distribution and evolution of gap distances along the contact boundaries. At the end of cooling in the 1st cycle (t=1800s), a maximal radial gap distance of 0.64mm for edge-on configuration and a 1.99mm poloidal gap for layer configuration are found, as shown in Fig. 7. The discrepancy in gap distances formed is due to the difference sizes in the two geometries. Thus, the pebble bed/wall gap distance can be reduced through the optimized geometry design of pebble bed container. Gap distance also varies with location for both configurations.

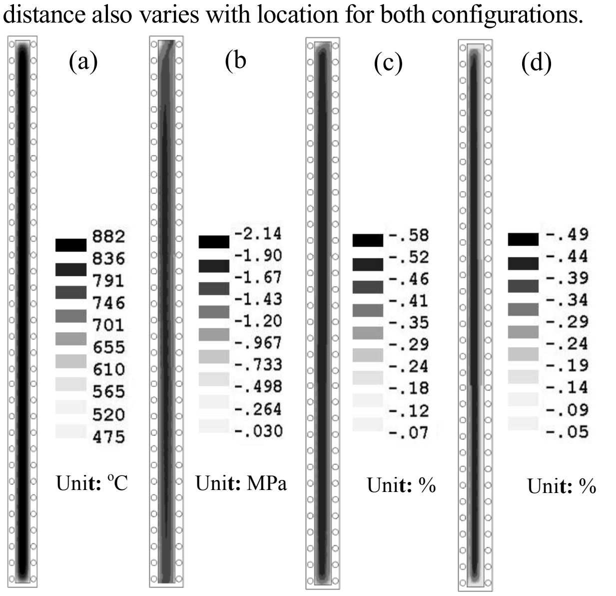

Fig. 5. Thermomechanical field distribution of Li_4SiO_4 pebble bed at the end of 1st heating period (t=400s) for layer configuration: (a) temperature; (b) poloidal stress; (c) poloidal plastic strain; (d) poloidal creep strain.

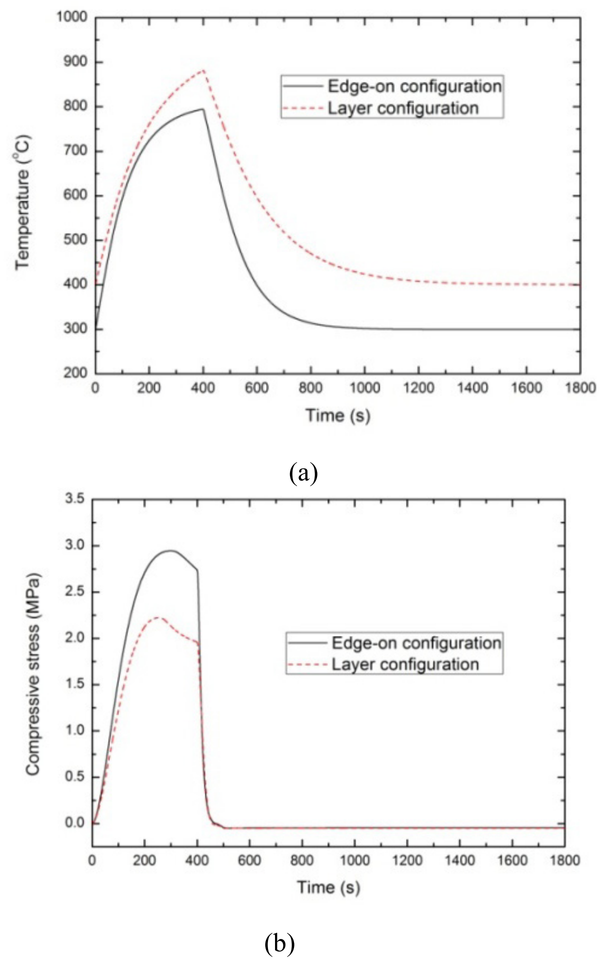

Fig. 6. Evolution of the 1st ITER cycle at Positions A/D: (a) temperature; (b) radial stress for edge-on configuration and poloidal stress for layer configuration.

By comparison, the larger gap in the layer configuration is related with its greater inelastic deformation of the pebble bed, shown in Figs. 4 and 5. The difference of major gap location for two configurations may result in different reduction extents of pebble bed/wall heat transfer efficiency. The major gap in edge-on configuration is located on the short edge far away from the FW, while that in the layer configuration is on the top of pebble bed in the poloidal direction. Considering the larger magnitude of gap distance in layer configuration, further pebble rearrangement can occur due to the existence of the gap. For example, pebbles will rearrange in the packing to fill lower gaps in the poloidal direction driven by the internal forces and gravity, especially when the gap distance is larger than pebble's diameter. Detailed discussions can be found in Section III.C.

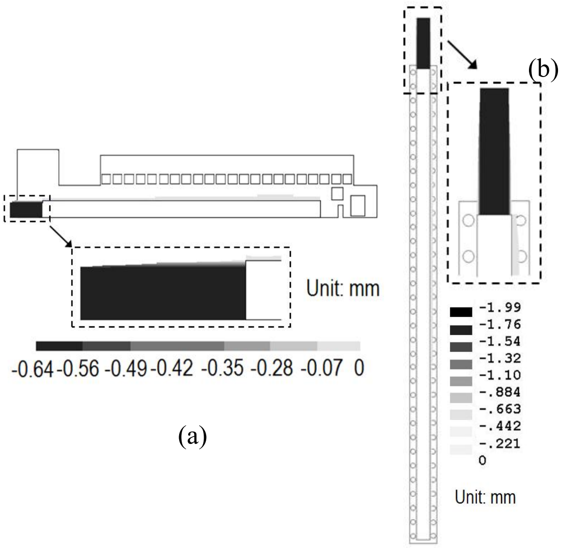

Fig. 7. Gap distance distribution at the end of the 1st ITER cycle (t=1800s): (a) edge-on configuration; (b) layer configuration.

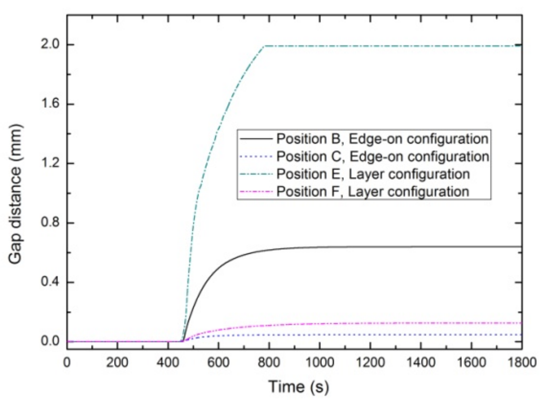

Fig. 8. Gap distance evolution for the 1st ITER cycle at Positions B/C/E/F.

The pebble bed/wall separation process can be described in the following sequence: 1) The pebble bed is compressed by structural walls due to temperature rise and their CTEs (coefficient of thermal expansion) differences; 2) The compressive stress from the structural wall results in an irrecoverable pebble bed volume reduction through inelastic deformation; 3) During the cooling period, pebble bed/wall separation is generated when pebble bed's dimension is smaller than the container at some particular time and position. In Fig. 8, we see the evolution of pebble bed/wall separation for both configurations, which starts at about 450s, and then the gap distance increases with time and saturates at about 800s.

Simulation results have also shown that pebble bed/wall separation and contact are a dynamic process, illustrated in Fig. 9. The generated gap, e.g. along Path G-H, in the 1st cycle can be closed during the 2nd heating period (t=1900s) due to pebble bed thermal expansion, and occur again during the 2nd cooling period (t=2300s). When the generated gap during the plasma-off period is small and closed during next plasma-on period, it does not have much effect on heat transfer capability. The CTE of pebble bed plays a key role in determining such dynamic behavior, e.g. the gap caused by pebble bed volume reduction (or inelastic deformation) will be closed or remain open. Therefore, further experimental study on pebble bed CTE measurement is suggested since it also determines the stress/strain level among pebble bed.

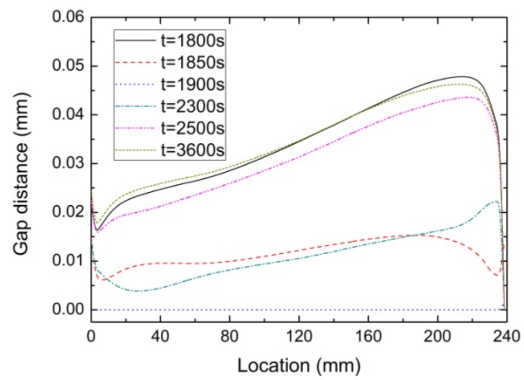

Fig. 9. Gap distance evolution for the 2nd ITER cycle and edge-on configuration along Path G-H.

III.C. Discussions

Simulation results presented above show that a pebble bed volume reduces more in a layer configuration than in an edge-on configuration within the range of studied parameters. Thus, a larger pebble bed/wall gap is found in the layer configuration. Conversely, the peak stress in the edge-on configuration is larger than in the layer configuration, though the generated stresses in both configurations should not be high enough to cause pebble cracking.

The pebble bed/wall gap distance and its dynamic process shown in Figs. 7-9 are obtained mainly based on the thermal expansion/contraction of the pebble bed and structural container, which does not consider the effect of further pebble rearrangement due to gap generation. Since the driving forces for such rearrangement are the gravity and imbalanced pebble bed internal forces, the gap distance predicted by FEM simulation can be changed in the way of: 1) closing the gaps at the lower poloidal positions; 2) generating additional gaps at the higher poloidal positions while conserving volume of the pebble region. Considering the dimensions for both configurations, after pebbles further rearrange, the layer configuration will have an even larger gap, while a thin gap layer will result on the top of pebble bed (poloidal direction) for the edge-on configuration.

As discussed, the pebble bed/wall separation strongly depends on pebble bed inelastic deformation during the heating period. To minimize the gap distance and reduction of heat transfer efficiency, the permanent pebble bed volume reduction (or inelastic strain in FEM simulation) during operation should be well controlled. The suggested ways to achieve such a goal are: 1) obtaining a well-packed pebble bed condition in pebbles filling process by both shaking and cyclic loading; 2) using sectional structural containers instead of a long sections, which can avoid the large gap generation and better restrain pebbles rearrangement and connected consequences.

IV. CONCLUSIONS

The phenomenon of pebble bed/structural wall separation has been studied with developed FEM models and compared for edge-on and layer configurations, as well as pebble bed thermomechanical behavior under ITER pulsed operation condition.

Pebble bed/wall separation, varying with their contact location, is mainly caused by and strongly dependent on pebble bed permanent volume reduction. Due to the cyclic pattern of ITER operation condition, a dynamic contact and separation process is found.

The peak gap distance is found on the short edge for both configurations, while the long edge has a much smaller gap. The layer configuration has a larger gap (1.99mm) than edge-on configuration (0.64mm) after the 1st ITER cycle within the range of studied parameters. Importantly, the poloidal gap of 1.99mm for layer configuration is larger than the pebble diameter, which will very likely cause more large pebble rearrangement.

The developed FEM model is able to aid the TBM design including the dimension and configuration optimization, and predict pebble bed behaviors of greatest concern to designers such as pebble bed creep and stress relaxation.

ACKNOWLEDGMENTS

This work was jointly supported by the U. S. Department of Energy Contract DE-FG03-ER52123.

REFERENCES

1. A. Ying, J. Reimann, L. Boccaccini, M. Enoeda, M. Kamlah, R. Knitter,Y. Gan, J. G. van der Laan, L. Magielsen, P. A. Di Maio, G. Dell'Orco, R. K. Annabattula, J. T. Van Lew, H. Tanigawa, S. van Til, "Status of Ceramic Breeder Pebble Bed Thermo-mechanics R&D and Impact on Breeder Material Mechanical Strength," *Fusion Engineering and Design*, **87**, 1130-1137 (2012); http://dx.doi.org/ 10.1016/j.fusengdes.2012.02.090.
2. Mechanical APDL Theory Reference, ANSYS release 14.0 (2011).
3. O. Coube, "Modelling and Numerical Simulation of Powder Die Compaction with Consideration of Cracking," *Ph.D. Theris*, University Pierre et Marie Curie, Paris VI (1988).
4. D. Hofer and M. Kamlah, "Drucker-Prager-Cap Creep Modelling of Pebble Beds in Fusion Blankets," *Fusion Engineering and Design*, **73**, 105-117 (2005); http://dx.doi.org/10.1016/j.fusengdes.2005.02.002.
5. D. Pelessone, "A Modified Formulation of the Cap Model," *Gulf Atomics Report GA-C19579 to the Defense Nuclear Angency* (1989).
6. A. F. Fossum and J. T. Fredrich, "Cap Plasticity Model and Compactive and Dilatant Prefailure Deformation," *Pacific Rocks 200: Rock Around the Rim, A. A. Balkema*, 1169-1176 (2000).
7. Y. Gan and M. Kamlah, "Identification of Material Parameters of a Thermomechanical Model for Pebble Beds in Fusion Blankets," *Fusion Engineering and Design*, **82**, 189-206 (2007); http://dx.doi.org/ 10.1016/j.fusengdes.2006.09.005.
8. J. Reimann and G. Wörner, "Thermal Creep of Li_4SiO_4 Pebble Beds," *Fusion Engineering and Design*, **58-59**, 647-651 (2001); http://dx.doi.org/ 10.1016/S0920-3796(01)00513-0.
9. M. Dalle Donnea, G. Piazzaa and A. Goraiebb, "Measurements of the Effective Thermal Conductivity of a Li_4SiO_4 Pebble Bed," *Fusion Engineering and Design*, **49-50**, 513-519 (2000); http://dx.doi.org/10.1016/S0920-3796(00)00261-1.
10. Y. Gan and M. Kamlah, "Thermo-mechanical Modelling of Ceramic Breeder Pebble Beds and Its Application in HELICA Mockup," *In CBBI-14: Fourteenth International Workshop on Ceramic Breeder Blanket Interactions*, Petten, The Netherlands (2006).
11. Y. Gan and M. Kamlah, "Thermo-mechanical Modelling of Pebble Bed/Wall Interfaces," *Fusion Engineering and Design*, **85**, 24-32 (2010); http://dx.doi.org/10.1016/j.fusengdes.2009.05.003.
12. A. Abou-Sena, A. Ying, and M. Abdou, "Effective Thermal Conductivity of Lithium Ceramic Pebble Beds for Fusion Blankets: A Review," *Fusion Science and Technology*, **47**, 1094-1100 (2005); http://dx.doi.org/10.13182/FST05-3.